



THREE-DIMENSIONAL IMAGING WITH STEREOTACTIC ULTRASONOGRAPHY

Jason W. Trobaugh, Darin J. Trobaugh, and William D. Richard*

Department of Electrical Engineering, Washington University of St. Louis, St. Louis, MO, USA

(Received 9 November 1993)

Abstract—Stereotactic ultrasonography is a technique for determining the position and orientation of B-mode ultrasound images in a reference coordinate system. A technique for constructing three-dimensional (3D) image volumes has been developed that uses this new technology. Given several registered images, a 3D volume is constructed either by a “nearest-neighbor” or a “closest-points” interpolation approach. The resulting volume can be rendered using 3D rendering software. In addition, the voxels in the volume are at known positions allowing determination of position for structures in the volume. Results are shown for various test cases, and applicability to medical imaging applications and stereotactic neurosurgery is discussed.

Key Words: Stereotactic ultrasonography, Interpolation, Nearest-neighbor, 3D rendering, Stereotactic neurosurgery

INTRODUCTION

Stereotactic ultrasonography has been recently developed as a technique for registering ultrasound images in a defined coordinate system (1–3). An optical position-sensing system is used to determine the positions of infrared LEDs with respect to a defined coordinate system (4). By affixing at least three LEDs to an ultrasound probe, the position in space of the ultrasound image produced by the probe can be determined with an accuracy of 1.5 mm (1, 2). An ultrasound probe configured for stereotactic use is shown in Fig. 1.

A three-dimensional (3D) image can provide useful information about an object such as its volume or shape (5–8). In addition, 3D rendering software can display images formed from a 3D volume for a more natural view than that available from the corresponding two-dimensional (2D) images. Most techniques for constructing the volume of data require significant mechanical precision to assure that the images are acquired in a known orientation. Typically, images are taken in parallel planes, and the images are stacked together to form a 3D volume (5, 6, 9). Most techniques used to form 3D volumes from ultrasound images require special probes (9) or special mechanisms that allow strict movement of the probe during acquisition of the images (5, 6, 9). The technique described here allows the formation of a 3D volume from images taken in any orientation. The only required equipment, in

addition to the ultrasound system, is a position-sensing system and a 3D rendering package.

In this technique, the relative orientation of the images does not have to be uniform because the volume is constructed with pixel information from the registered images. However, to form a volume truly representative of an object, images must be acquired that “cover” the entire volume. Any space in the volume uncovered by the images is filled using information from adjacent images. It is thus beneficial to take the images in a roughly organized manner. Two image orientations were used for the test cases. In one method, images are taken in approximately parallel planes separated by roughly equal distances. In a second method, images are taken in planes rotated through roughly equal angles about an axis through the center of the volume.

Two methods were developed to construct a 3D ultrasound volume from a set of 2D stereotactic images. In both methods, eight points are chosen to bound the volume so that the desired 3D region is contained, as shown in Fig. 2. By choosing the resolution of the volume, the size of each voxel is determined. A brightness value for each voxel must then be determined. The first method uses a “nearest-neighbor” approach. Each registered image is processed by assigning the brightness value of each image pixel to the nearest voxel in the volume. Voxels not “colored” by this method are left blank so that this volume can be viewed to determine the relative orientation of the images. The second method is an interpolation approach. For each voxel in the volume, a brightness value is interpolated from the two closest images that surround the voxel. If no

* Correspondence should be addressed to William D. Richard, Ph.D., Department of Electrical Engineering, Washington University of St. Louis, Campus Box 1127, 1 Brookings Drive, St. Louis, MO 63130.



Fig. 1. Ultrasound probe configured for stereotactic use.

two planes surround the voxel, it is outside the region “covered” by the images, and it is left blank.

The next section describes the two volume construction methods. Results for test objects are then shown demonstrating the effectiveness of the technique for both image acquisition methods described above. In the final section, the technique and possible applications, including its use in stereotactic neurosurgery, are discussed.

METHODS

The problem of creating a 3D volume can be stated as follows: given a set of stereotactically located images of arbitrary position, construct a 3D volume that represents the registered image information. For each acquired stereotactic image, registration consists of defining the following equation:

$$\begin{bmatrix} x_{pt} \\ y_{pt} \\ z_{pt} \end{bmatrix} = \begin{bmatrix} x_{st} \\ y_{st} \\ z_{st} \end{bmatrix} + \begin{bmatrix} x_{rt} \\ y_{rt} \\ z_{rt} \end{bmatrix} * x_{us} + \begin{bmatrix} x_{up} \\ y_{up} \\ z_{up} \end{bmatrix} * y_{us}, \quad (1)$$

or

$$\begin{bmatrix} x_{pt} \\ y_{pt} \\ z_{pt} \end{bmatrix} = \begin{bmatrix} x_{st} & x_{rt} & x_{up} \\ y_{st} & y_{rt} & y_{up} \\ z_{st} & z_{rt} & z_{up} \end{bmatrix} * \begin{bmatrix} 1 \\ x_{us} \\ y_{us} \end{bmatrix}, \quad (2)$$

or

$$pt = A * us, \quad (3)$$

where (x_{pt}, y_{pt}, z_{pt}) are the 3D coordinates of pixel (x_{us}, y_{us}) in the 2D image. The lower left-hand corner in the ultrasound image is at (x_{st}, y_{st}, z_{st}) , and (x_{rt}, y_{rt}, z_{rt}) and (x_{up}, y_{up}, z_{up}) are 3D vectors that define the distance to move one pixel right in the image and one pixel up in the image, respectively. These coordinates are based on a reference coordinate system and have dimensions

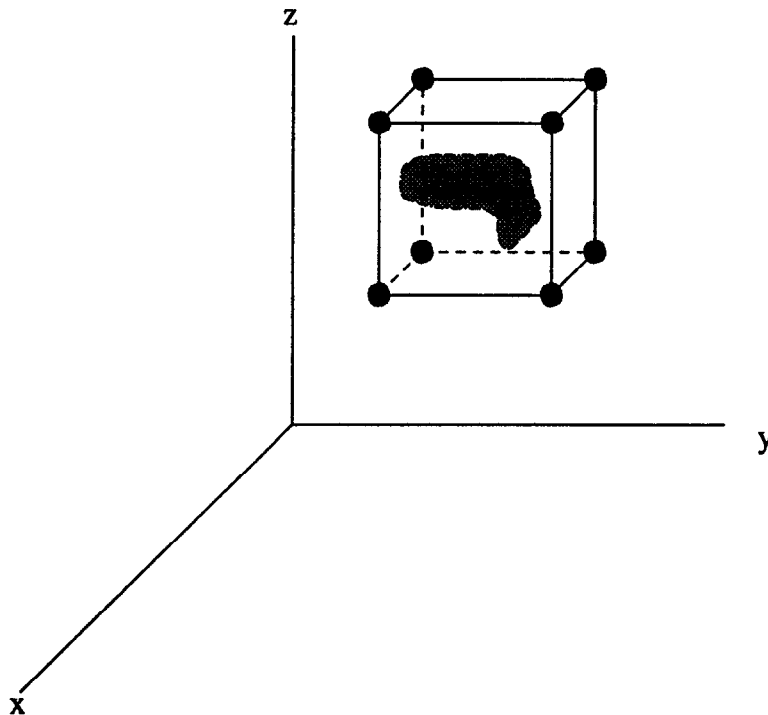


Fig. 2. Eight points are chosen to bound the volume to be constructed.

of millimeters. Each image pixel has an exact voxel coordinate position in the bounded volume given by:

$$(x_{vox}, y_{vox}, z_{vox}) = \left(\frac{x_{pt} - x_{volst}}{x_{size}}, \frac{y_{pt} - y_{volst}}{y_{size}}, \frac{z_{pt} - z_{volst}}{z_{size}} \right), \quad (4)$$

where $(x_{volst}, y_{volst}, z_{volst})$ are the real coordinates of the lower-left corner of the volume, and x_{size} , y_{size} , and z_{size} are the dimensions of the voxel, in millimeters.

Nearest-neighbor construction

In the nearest-neighbor approach, information from each registered image is placed into the volume at the closest corresponding location. Specifically, for each nonzero pixel, the following routine is performed:

1. Calculate the corresponding voxel coordinate position for the pixel using (4).
2. Round the position to the nearest voxel.
3. Assign the pixel value to the voxel identified in step 2.

The volume is created by processing every pixel of each registered image in this fashion. This method is simple and executes quickly. Some voxels in the volume, however, are left blank unless the volume is heavily sampled.

Interpolation construction

The interpolation method is more complicated than the nearest neighbor approximation, but it leaves no voxel unfilled in the part of the volume covered by ultrasound data. In this approach, a brightness value for each voxel is determined based on the two closest registered images that surround the voxel. For a given voxel, the closest image is found. Then, the closest image on the opposite side of the voxel is found. If no two images surround the voxel, it lies outside the region covered by the registered images, and it is left blank.

In order to determine the closest distance from a voxel to each image, equations must be known that describe each registered image. Because the distance from a point to a plane can be easily found with the point-normal plane equation, this equation is determined for each image. The normal vector to the plane of an image is equal to the cross-product of the up and right vectors for that image, i.e.,

$$\begin{bmatrix} a \\ b \\ c \end{bmatrix} = \begin{bmatrix} x_{rt} \\ y_{rt} \\ z_{rt} \end{bmatrix} \times \begin{bmatrix} x_{up} \\ y_{up} \\ z_{up} \end{bmatrix}. \quad (5)$$

To complete the plane equation, a point in the plane is needed. The point from the lower-left corner of the image, i.e., (x_{st}, y_{st}, z_{st}) , can be chosen. If this choice is made, then

$$a(x - x_{st}) + b(y - y_{st}) + c(z - z_{st}) = 0, \quad (6)$$

or

$$ax + by + cz = d. \quad (7)$$

Once these plane equations are determined, the following steps are taken to determine the brightness value for each voxel, (x_v, y_v, z_v) , where $x_v \in \{0, 1, 2, \dots, x_{dim}\}$, $y_v \in \{0, 1, \dots, y_{dim}\}$, and $z_v \in \{0, 1, \dots, z_{dim}\}$ in the specified volume with dimensions $(x_{dim}, y_{dim}, z_{dim})$:

1. The perpendicular distance from the voxel to the plane of each image is calculated as the magnitude of D :

$$D = \frac{a \cdot x_{vmm} + b \cdot y_{vmm} + c \cdot z_{vmm} - d}{\sqrt{a^2 + b^2 + c^2}}, \quad (8)$$

where a , b , c , and d are from (7), and $(x_{vmm}, y_{vmm}, z_{vmm})$ are the coordinates of the voxel in millimeters.

2. The plane closest to the voxel is identified by choosing the one for which D is the smallest.
3. The closest image plane on the opposite side of the voxel is now desired. A normal vector is formed from the voxel to the image identified in step 2. For each other image, similar normal vectors are formed. The angle between each of these vectors and the vector to the image identified in step 2 determines whether the image is on the opposite side. Specifically, if the angle is greater than 90 degrees, the planes are on opposite sides of the voxel. The closest image on the *opposite* side is then identified by choosing from those images on the opposite side the one for which the value of D is smallest.
4. In each of the identified planes, the closest point to the voxel whose brightness is being calculated is found as follows:

$$(x_{pt}, y_{pt}, z_{pt}) = (x_{vox}, y_{vox}, z_{vox}) + \text{unit}(x_n, y_n, z_n) \cdot D, \quad (9)$$

where $\text{unit}(x_n, y_n, z_n)$ is the unit normal vector for the image.

5. Because each point is in the plane of the corresponding image, a pixel location in the image is determined as follows:

$$\begin{bmatrix} 1 \\ x \\ y \end{bmatrix} = A^{-1} \cdot \begin{bmatrix} x_{pt} \\ y_{pt} \\ z_{pt} \end{bmatrix}. \quad (10)$$

6. If this pixel number is within the bounds of the image, i.e., $0 < x < 256$, $0 < y < 256$, the four surrounding pixels are located, and a brightness is bilinearly interpolated using those pixel values which are not equal to zero.

7. A brightness for the voxel is then interpolated as a weighted sum based on the distances from the voxel to the two planes.

The procedure is then repeated for each voxel in the specified volume.

RESULTS

Ultrasound images were taken with a Linscan Systems, Inc., Intrascan B-mode ultrasound system and stereotactically registered using the method documented (1–3) with a Pixsys, Inc., optical position-sensing system. Both 7.5-MHz and 10-MHz standard B-mode ultrasound probes were used to form ultrasound images of various test objects. A modified ultrasound system was used which allowed images to be saved on a standard floppy disk. To obtain parallel images, a simple screw-driven probe positioner was constructed. The probe was moved manually using the positioner, and images were saved at roughly equal distance increments. To obtain images radially, a plastic cylinder open on top and partially open on the bottom was clamped to a metal stand. The probe rested in this cylinder, and images were saved as it was rotated through approximately equal angles.

Software was written in C and run on a Sun SPARCstation 1 to form 3D volumes using the two methods described above. Rendered images were created from the volumes using a commercial rendering package (10) on a Silicon Graphics 240 VGX machine.

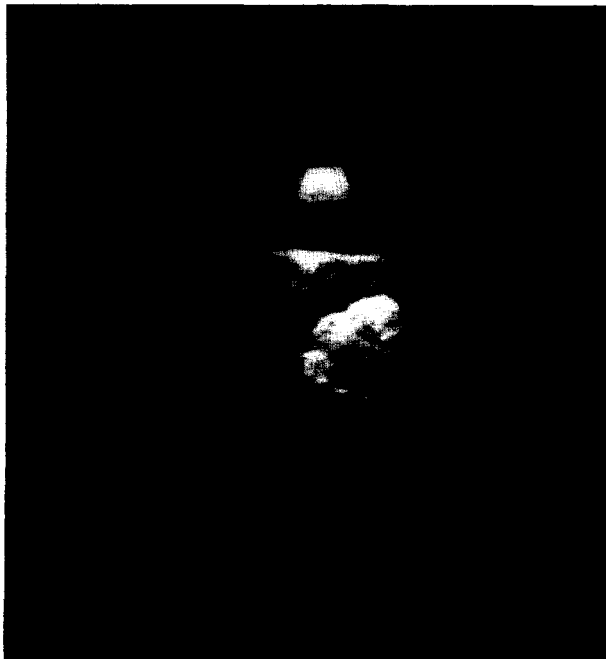


Fig. 3. Sample ultrasound image of canine brain.

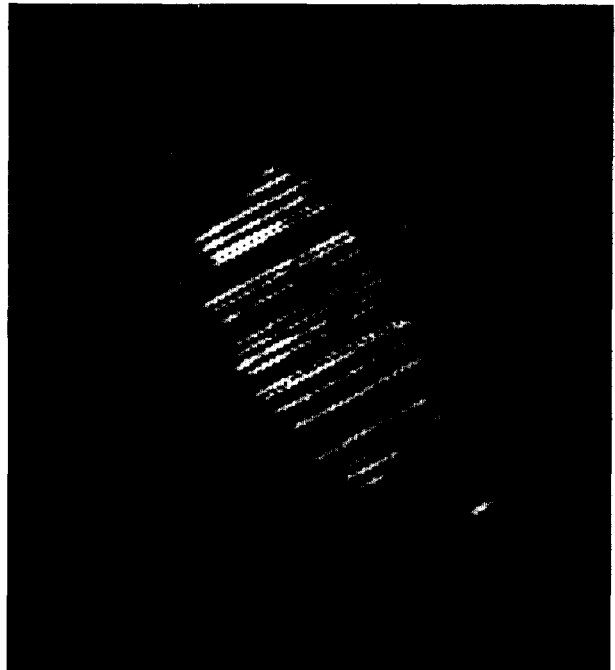


Fig. 4. Slice from nearest-neighbor volume for canine brain.

The first test object was one hemisphere of a canine brain suspended in gelatin. The screw-driven positioner was used to move the probe. Fifty images spaced approximately 1.5 mm apart were acquired. One of these images is shown in Fig. 3. The roughly horizontal line



Fig. 5. Slice from interpolated volume for canine brain.



Fig. 6. Rendering of nearest-neighbor 3D volume of canine brain.

near the top of the image is a reflection from the water-gelatin interface. The image shows only the top portion of the brain due to the high attenuation of the ultrasonic pulse as it traveled through the brain. Three-dimensional volumes were created using the nearest-neighbor and interpolation approaches. The size of each volume is $128 \times 128 \times 50$ voxels. This volume can be viewed as 50 parallel 128×128 images. A sample slice from the nearest-neighbor volume is shown in Fig. 4. This image shows the relative orientation of the registered images, since it represents a plane perpendicular to the registered images. A slice from the interpolated volume is shown in Fig. 5. This image shows the interpolation that has occurred between the registered images. The rendering of the nearest-neighbor volume is shown in Fig. 6, and the rendering of the interpolated volume is shown in Fig. 7. In the nearest-neighbor volume, the individual slices are apparent, whereas the space between images has been filled in the interpolated volume. Some "noise" from the water-gelatin interface can be seen at the top of the rendering.

A second study was done using the radial positioning method on two olives suspended in water. Thirty-five localized images were taken, and a $128 \times 128 \times 50$ -voxel volume was created. Samples of the constructed volume slices using the nearest-neighbor and interpolation methods are shown in Figs. 8 and 9, respectively. Fig. 8 shows the relative orientation of the images, and Fig. 9 shows the interpolation between the registered images. The corresponding rendered 3D im-

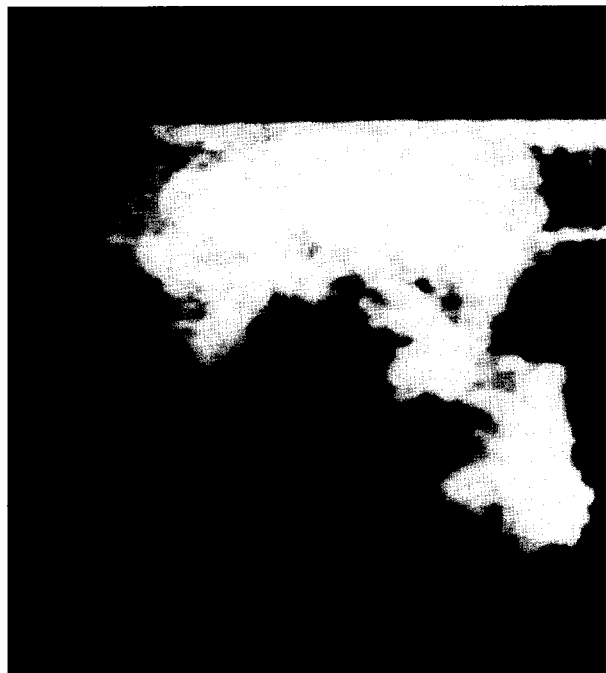


Fig. 7. Rendering of interpolated 3D volume of canine brain.

ages are shown in Figs. 10 and 11. These renderings show how the space in the nearest-neighbor volume is filled in the interpolated volume.

To compare the two orientation methods, images were acquired of a rabbit brain suspended in water.



Fig. 8. Slice from nearest-neighbor volume for suspended olives.

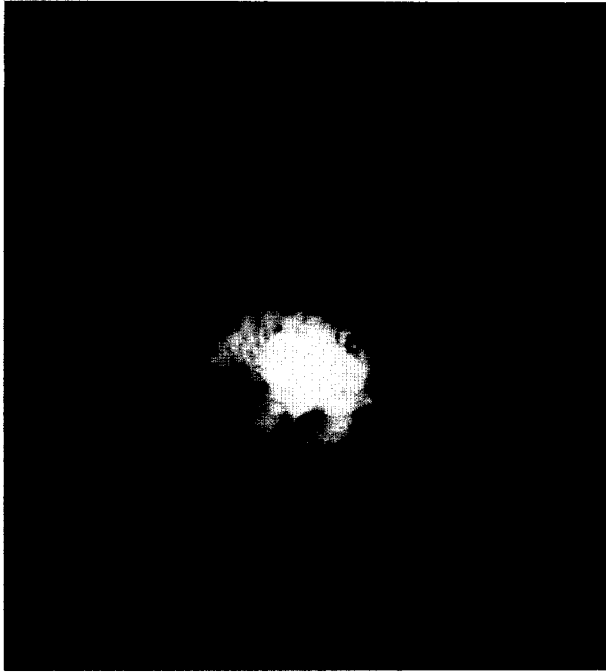


Fig. 9. Slice from interpolated volume for suspended olives.

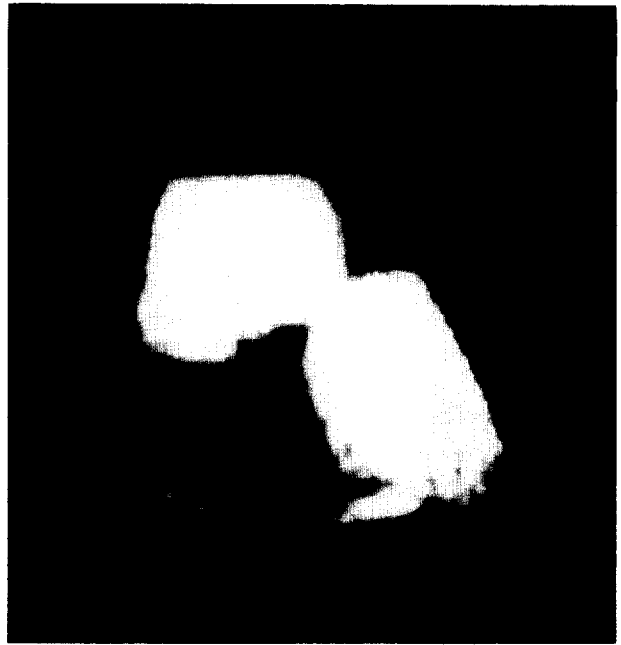


Fig. 11. Rendering of interpolated 3D volume of suspended olives.

Fifteen images were taken using the radial method, and 35 images were taken using the parallel method. The interpolation method was used to construct both volumes. Figs. 12 and 13 show sample images from

the two volumes. The sample from the volume constructed using the radial method contains less detail than that constructed with the parallel method. This is a result of the number of images used to construct each volume. More interpolation was required to fill

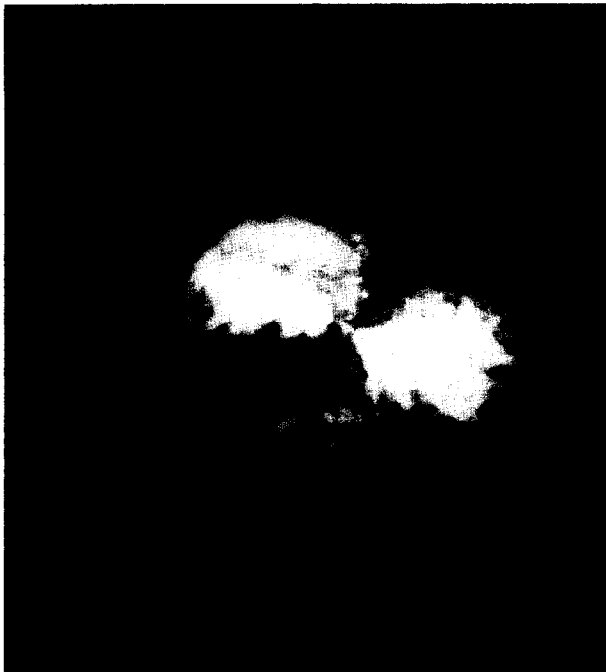


Fig. 10. Rendering of nearest-neighbor 3D volume of suspended olives.



Fig. 12. Slice from radial method with rabbit brain.



Fig. 13. Slice from parallel method with rabbit brain.



Fig. 14. Rendered volume of rabbit brain using the radial method.

in the space between the registered images in the volume constructed using the radial method. Figs. 14 and 15 show renderings of the two 3D volumes. The difference between the two methods is much less apparent in the 3D renderings than in the 2D images.

DISCUSSION

The nearest-neighbor technique is the simpler of the two techniques and would work well given enough images to adequately represent the object. With fewer images, the linear interpolation technique provides a 3D volume which can be rendered to give a 3D view of the object. However, the interpolation technique is computationally intensive in comparison with the nearest-neighbor technique. For the canine brain shown in Figs. 3–7, the nearest-neighbor algorithm required approximately 2 seconds to process each image for a total of 3 minutes of CPU time (including disk access time) on a SUN SPARCstation 1, whereas the interpolation algorithm required over 45 minutes. The code written to implement these algorithms has not been optimized in any way.

The simplicity of the nearest-neighbor method is its greatest advantage. This method could be used to provide near real-time creation of a 3D volume. Current use of this method is limited by the rate at which the ultrasound images can be saved. It takes approximately 40 seconds to transfer one image from the ultrasound machine to floppy disk. However, with spe-

cial-purpose hardware, the ultrasound images could be processed in near real-time and added to the volume as they are created with no limit on the number of



Fig. 15. Rendered volume of rabbit brain using the parallel method.

images to be included. As the user scans the object, the received information could simply be added to the 3D volume. Voxel values could be averaged over all received information or could maintain the same value once "colored."

If the object cannot be imaged so as to fully "color" the volume, some interpolation is required between images. The method used here could be simplified if the orientation of the images were known. The two closest images surrounding each voxel would still have to be known, but all images would not have to be checked. By constraining the way in which images are acquired, e.g., by acquiring images in a translationally or rotationally sequential manner, only two images would need to be checked to form each voxel. This would significantly reduce the computational cost associated with the interpolation algorithm. For images of the size used here, the time required to form the 3D volume would decrease by approximately an order-of-magnitude.

Applications for the technique include use in the frameless stereotactic neurosurgery technique now being developed (11–14). Stereotactic ultrasound has been used to provide a real-time ultrasound image which can be compared with an oblique CT/MR image reconstructed from a preoperative volume of computed tomography (CT) or magnetic resonance (MR) images. In the current implementation, the corresponding oblique CT/MR images are created at a rate of approximately three per second, although near real-time operation will be possible with improved interface hardware. From the comparison of the images, an assessment of the intraoperative shift in intracranial structures can be made (1, 2). By constructing a 3D volume of ultrasound data through a small burr hole, shift assessment could be made for the entire volume of CT/MR images. Research is under way in the application of template deformation techniques (15) to automate shift assessment and correction.

Other possibilities for medical applications also exist. A system of this type could be used to image patients with detached retinas so that 3D surgical planning could be performed. By imaging the prostate or other abdominal organs, the accuracy of radiation treatment could be improved. Currently, patients are imaged with CT or MR and moved to a radiation treatment system. The organs to receive radiation therapy, i.e., the prostate, kidneys, or liver, shift during the transfer. A system of the type described above for stereotactic shift assessment in neurosurgery could be used to register the organs after the patient has been moved.

CONCLUSIONS

Although techniques exist for the construction of 3D ultrasound images, the advantage of using stereo-

tactic ultrasound as described here to create 3D images is the simplicity of the method and of the required equipment. Using this method, 3D images can be created using a standard ultrasound system in conjunction with localization equipment and a workstation with 3D rendering software. With this technique, the relative orientation of the acquired images does not have to be uniform, and the spacing between images does not have to be exact because the location of each image is known. Possible uses for the method include its use for shift assessment in stereotactic neurosurgery and other 3D imaging applications ranging from ophthalmic to prostatic.

SUMMARY

This article describes a new method that can be used to construct a three-dimensional (3D) ultrasound volume. The method utilizes a recently developed technique for registering ultrasound images in a 3D coordinate system. By registering several images, the 3D volume can be constructed based on the registered images regardless of their orientation. The method is simple and allows construction of the volume with a variety of methods. Two methods are described here. The first method, a nearest-neighbor approach, simply assigns every pixel in the registered image to the closest voxel. A second method interpolates between the two closest images to determine the brightness of each voxel. In addition, two methods of image orientation are described. The images can be taken in a parallel fashion, or radially; i.e., rotated around a central axis.

Results are shown for some test objects, and images are displayed which demonstrate the effectiveness of the technique and show the differences between some of the methods. The two construction methods are discussed with the advantages and disadvantages to each. Application to stereotactic neurosurgery is stressed.

Acknowledgments—We would like to extend our appreciation to Linscan Systems, Inc., of Rolla, Missouri, for the use of their ultrasonic equipment in this research project, and to Dr. Richard Bucholz at the St. Louis University School of Medicine for his cooperation and assistance in using the stereotactic equipment. Jason Trobaugh was funded by a fellowship grant from the Department of Education.

REFERENCES

1. Trobaugh, J.W.; Richard, W.D.; Smith, K.R.; Bucholz, R.D. Frameless stereotactic ultrasonography: Method and applications. *Comput. Med. Imag. Graphics* 18(4):235–246; 1994.
2. Trobaugh, J.W. Frameless stereotactic ultrasonography in neurosurgery. M.S. Thesis, Washington University of St. Louis, May 1993.
3. Bucholz, R.D.; Trobaugh, J.W.; Richard, W.D. Three-dimensional intraoperative ultrasonography using an optical digitizer [abstract]. *Proc. of the 61st AANS Annual Meeting* 61:149; 1993.

4. Macellari, V. A computer peripheral remote sensing device for 3-dimensional monitoring of human motion. *Med. Biol. Eng. Comput.* 21:311-318; 1983.
5. Nakamura, S. Three-dimensional digital display of ultrasonograms. *IEEE Comp. Graphics Appl.* 4:36-45; 1984.
6. Nakamura, S. Monitoring of the three-dimensional prostate shape under anti-androgen therapy. *Diagnostic ultrasound of the prostate. Proc. 1st Int. Workshop on Diagnostic Ultrasound of the Prostate.* 1988: 137-144.
7. Ledley, R.S.; Golab, T.J.; Buas, M.; Arminski, L. True 3-D stereo ultrasonography to make ultrasound more easily understood. *Proc. 12th Annual Int. Conf. of the IEEE Engineering in Medicine and Biology Society, Philadelphia, PA* 12:211-212; Nov 1-4, 1990.
8. Ledley, R.S.; Collea, J.V. Stereo ultrasonography in obstetrics. *Radiological Society of North America, 77th Scientific Assembly and Annual Meeting, Chicago, IL, Dec 1-6 1991, Vol. 181(P)* (supplement to *Radiology*, Nov. 1991, p. 132).
9. Richard, W.D.; Grimmell, C.K.; Bedigian, K.; Frank, K.J. A Method for three-dimensional prostate imaging using transrectal ultrasound. *Comput. Med. Imag. Graphics* 17:73-79; 1993.
10. Holden, P. *VoxelView, an interactive volume rendering system.* Fairfield, IA: Vital Images, Inc.; 1991.
11. Smith, K.R.; Bucholz, R.D. Computer methods for improved diagnostic image display applied to frameless stereotactic neurosurgery. *Automedica* 14:371-382; 1992.
12. Guthrie, B.L.; Adler, Jr., J.R. Computer-assisted preoperative planning, interactive surgery, and frameless stereotaxy. In: *Clinical neurosurgery.* Baltimore: Williams & Wilkins; 1990: 112.
13. Bucholz, R.D. System for indicating the position of a surgical probe within a head on an image of the head. U.S. Patent Pending, Application S.N. 07/600,753.
14. Smith, K.R.; Henderson, J.M.; Trobaugh, J.W.; Richard, W.D.; Frank, K.J.; Bucholz, R.D. Registration methods for frameless stereotactic neurosurgery. *IEEE Trans. Med. Imag.* (in press).
15. Amit, Y.; Grenander, U.; Piccioni, M. Structural image restoration through deformable templates. *J. Am. Stat. Assoc.* 86: 376-87; June 1991.

About the Author—JASON W. TROBAUGH received his M.S.E.E. and is currently working on his D.Sc. at Washington University in St. Louis. His research interests include ultrasonic imaging and image processing.

About the Author—DARIN J. TROBAUGH is in his junior year at the University of Illinois at Champaign-Urbana working on an undergraduate engineering degree.

About the Author—WILLIAM D. RICHARD received his Ph.D. from the University of Missouri-Rolla and joined the faculty at Washington University in St. Louis in 1988. His research interests include ultrasonic imaging and medical instrumentation.